



**HAL**  
open science

## **Lignin from oil palm empty fruit bunches: Characterization, biological activities and application in green synthesis of silver nanoparticles**

Luis Alberto Zevallos Torres, Adenise Lorenci Wociciechowski, Valcineide Oliveira de Andrade Tanobe, Arion Zandoná Filho, Rilton Alves de Freitas, Miguel Daniel Nosedá, Erico Saito Szameitat, Craig Faulds, Pedro Coutinho, Emanuel Bertrand, et al.

### ► **To cite this version:**

Luis Alberto Zevallos Torres, Adenise Lorenci Wociciechowski, Valcineide Oliveira de Andrade Tanobe, Arion Zandoná Filho, Rilton Alves de Freitas, et al.. Lignin from oil palm empty fruit bunches: Characterization, biological activities and application in green synthesis of silver nanoparticles. *International Journal of Biological Macromolecules*, 2021, 10.1016/j.ijbiomac.2020.11.104 . hal-03008866

**HAL Id: hal-03008866**

**<https://amu.hal.science/hal-03008866>**

Submitted on 17 Nov 2020

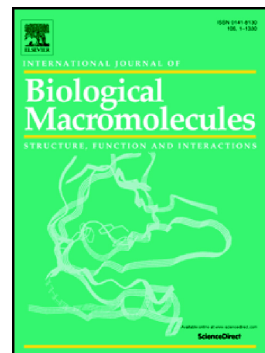
**HAL** is a multi-disciplinary open access archive for the deposit and dissemination of scientific research documents, whether they are published or not. The documents may come from teaching and research institutions in France or abroad, or from public or private research centers.

L'archive ouverte pluridisciplinaire **HAL**, est destinée au dépôt et à la diffusion de documents scientifiques de niveau recherche, publiés ou non, émanant des établissements d'enseignement et de recherche français ou étrangers, des laboratoires publics ou privés.

## Journal Pre-proof

Lignin from oil palm empty fruit bunches: Characterization, biological activities and application in green synthesis of silver nanoparticles

Luis Alberto Zevallos Torres, Adenise Lorenci Wociciechowski, Valcineide Oliveira de Andrade Tanobe, Arion Zandoná Filho, Rilton Alves de Freitas, Miguel Daniel Nosedá, Erico Saito Szameitat, Craig Faulds, Pedro Coutinho, Emanuel Bertrand, Carlos Ricardo Soccol



PII: S0141-8130(20)35032-7

DOI: <https://doi.org/10.1016/j.ijbiomac.2020.11.104>

Reference: BIOMAC 17267

To appear in: *International Journal of Biological Macromolecules*

Received date: 1 September 2020

Revised date: 12 November 2020

Accepted date: 14 November 2020

Please cite this article as: L.A.Z. Torres, A.L. Wociciechowski, V.O. de Andrade Tanobe, et al., Lignin from oil palm empty fruit bunches: Characterization, biological activities and application in green synthesis of silver nanoparticles, *International Journal of Biological Macromolecules* (2018), <https://doi.org/10.1016/j.ijbiomac.2020.11.104>

This is a PDF file of an article that has undergone enhancements after acceptance, such as the addition of a cover page and metadata, and formatting for readability, but it is not yet the definitive version of record. This version will undergo additional copyediting, typesetting and review before it is published in its final form, but we are providing this version to give early visibility of the article. Please note that, during the production process, errors may be discovered which could affect the content, and all legal disclaimers that apply to the journal pertain.

## **Lignin from oil palm empty fruit bunches: characterization, biological activities and application in green synthesis of silver nanoparticles**

Luis Alberto Zevallos Torres<sup>1</sup>; Adenise Lorenci Wociciechowski<sup>1</sup>; Valcineide Oliveira de Andrade Tanobe<sup>1</sup>; Arion Zandoná Filho<sup>2</sup>; Rilton Alves de Freitas<sup>3</sup>; Miguel Daniel Noseda<sup>4</sup>; Erico Saito Szameitat<sup>5</sup>; Craig Faulds<sup>6</sup>; Pedro Coutinho<sup>7,8</sup>; Emanuel Bertrand<sup>6</sup>; Carlos Ricardo Soccol<sup>1\*</sup>

<sup>1</sup>Bioprocess Engineering and Biotechnology Department, Federal University of Paraná, Brazil, Centro Politécnico, CP 19011, Curitiba-PR, 81531-908, Phone number: 005541 33613271

<sup>2</sup>Chemical Engineering Department, Federal University of Paraná, Brazil, Centro Politécnico, CP 19011, Curitiba-PR, 81531-908, Phone number: 005541 33613574

<sup>3</sup>Department of Chemistry, Federal University of Paraná, Brazil, Centro Politécnico, CP 19011, Curitiba-PR, 81531-908, Phone number: 005541 33613260

<sup>4</sup>Department of Biochemistry, Federal University of Paraná, Centro Politécnico, CP 19046, Curitiba, Brazil, 81531-980, Phone number: 005541 33611663

<sup>5</sup>Electron Microscopy Center, Federal University of Paraná, Brazil, Centro Politécnico, CP 19011, Curitiba-PR, 81530-001 Phone number: 005541 33613493

<sup>6</sup>INRAE, Aix Marseille Univ, BBr7, 13009, Marseille, France

<sup>7</sup>CNRS, Aix Marseille Univ, UMR7257, Marseille, France

<sup>8</sup>INRAE, USC1408, AFM3, Marseille, France

\*Corresponding author. E-mail address: soccol@ufpr.br (C.R. Soccol).

## Abstract

Lignin was extracted from oil palm empty fruit bunches under four different conditions. The lignin samples were characterized and employed in the green synthesis of silver nanoparticles. Two-dimensional HSQC NMR analysis showed that lignins extracted under more aggressive conditions (3.5% acid, 60 min) exhibited less signals and thus, presented a more degraded chemical structure. Additionally, those lignins obtained under harsh conditions (3.5% acid, 60 min) exhibited higher antioxidant capacity than those obtained under mild conditions (1.5% acid, 20 min). Formation of lignin-mediated silver nanoparticles was confirmed by color change during their synthesis. The surface plasmon resonance peaks (423-427 nm) in UV-visible spectra also confirmed the synthesis of AgNPs. AgNPs showed spherical shape, polycrystalline nature and average size between 18 and 20 nm. AgNPs, in suspension, presented a negative Zeta potential profile. Lignin was assumed to contribute in the antioxidant capacity exhibited by AgNPs. All AgNPs presented no significant differences on the disk diffusion antimicrobial susceptibility test against *E. coli*. The minimum inhibitory concentration of HAL3-L AgNPs ( $62.5 \mu\text{g}\cdot\text{mL}^{-1}$ ) was better than other physicochemically produced AgNPs ( $100 \mu\text{g}\cdot\text{mL}^{-1}$ ).

**Keywords:** Oil palm empty fruit bunches; lignin; silver nanoparticles.

## 1. INTRODUCTION

Oil palm (*Elaeis guineensis*) is grown as a plantation crop in most tropical climates countries with high rainfall, principally for processing the palm fruits to obtain edible and technical oils. Brazil represents the third producer in South America, with an annual production of 410,000 metric tons [1]. It is estimated that approximately 100 tons of fresh fruit bunches (FFB) can generate 20-22 tons of oil palm empty fruit bunches (OPEFB),

which are mainly composed by 30.5% of cellulose, 19.5% of hemicellulose and 32.17% of acid insoluble lignin [2,3].

The lignin, present in lignocellulosic biomass, is a three-dimensional amorphous macromolecule composed by crosslinked phenylpropanoid structures of sinapyl, coniferyl and *p*-coumaryl alcohols which give rise to the syringyl (S), guaiacyl (G) and *p*-hydroxyphenyl (H) lignin units, respectively [4]. This natural macromolecule, considered a residue from the pulp and paper industry, exhibits a great potential for many applications, including in the field of nanotechnology.

Currently, nanotechnology is a growing research area that support diverse industries, such as pesticides, electronics and medicine, providing a platform for collaboration in the fields of material and biological science [5]. Specifically, the synthesis of silver nanoparticles (AgNPs) have received significant interest because of their unique electrical, optical [6], catalytic [7], sensing [8] and even antimicrobial properties [9]. Their synthesis was traditionally done by chemical and physical methods. Subsequently, the toxicity of the reagents used in classical synthesis encouraged researchers to look for green synthesis methods, which involved the use of microorganisms [10–12], natural products or plant extracts such as essential oils [13], caffeic acid [14], polyhydroxyalkanoates [15], or even hydro-alcoholic extract from *Coffea arabica* seed [16].

Lignin, has already been shown a relatively high redox potential [17] and possesses the potential to bio-reduce silver ions for AgNPs synthesis. In this sense, a commercial Alkali lignin and lignin extracted from *Acacia* wood powder have been reported as reducing agents in the synthesis of AgNPs [18,19].

The aim of the present work was to take advantage of OPEFB as an agricultural waste and to develop a value-added lignin fraction. Sequential acid-alkaline pretreatment was

employed to obtain different lignin fractions which were further physicochemically characterized. Sequentially, the different lignin samples obtained from OPEFB were evaluated and compared in the green synthesis of AgNPs for the first time. The lignin-mediated AgNPs were then characterized and tested as possible antioxidant and antimicrobial agents.

## 2. EXPERIMENTAL

### 2.1. Isolation of lignin from oil palm empty fruit bunches

OPEFB was obtained from Biopalm Vale factory, located in Mojú (Pará), Brazil. OPEFB was dried in an air-circulating oven at 65°C for 48 h and milled in a knife-mill (Marconi, MA580/E). The particle size used in the experiments ranged between ASTM No. 20 (0.85 mm) and ASTM No. 45 sieves (0.35 mm). Lignin was extracted applying a sequential acid-alkaline pretreatment as described by other authors but with some modifications [3,17].

Briefly, OPEFB was first submitted to a dilute acid pretreatment in the conditions detailed on **Fig. 1**. A solid-liquid ratio of 10 wt.% was employed. The resulting product from dilute acid pretreatment was filtered using Whatman filter paper No. 40. The solid fraction was washed twice with deionized water to remove the excess of acid and carbohydrates and then, dried at 45°C for 24 h. After that, the dried solid fraction was submitted to alkaline extraction process in autoclave at 121°C for 60 min. A solid-liquid ratio of 2.5 wt.% and 10 wt.% of NaOH were employed. The liquid fraction (containing the extracted lignin) was acidified with 72 wt.% H<sub>2</sub>SO<sub>4</sub> until pH 2.0 and then filtered using Whatman filter paper No. 40. The precipitate was washed three times with an acidified water and followed by three washes with hot water. Finally, the washed lignin was dried at

80°C for 8 h. For all the experiments using lignin in a solubilized form, the dried lignin samples were solubilized in alkaline water (pH 11) under magnetic stirring at 80°C. After complete solubilization of lignin, the pH of the resulting solution was adjusted to 6-7 using 2 wt.% H<sub>2</sub>SO<sub>4</sub>.

## 2.2. Silver nanoparticles synthesis.

A 200 µg.mL<sup>-1</sup> lignin solution (Solution I) and a 20 mmol.L<sup>-1</sup> silver nitrate solution (Solution II) were prepared. Then, a certain volume from each solution (I and II) was taken, and diluted, to obtain the final concentrations of lignin and silver nitrate in the reaction mixture of 40 µg.mL<sup>-1</sup> and 2 mmol.L<sup>-1</sup>, respectively. The reaction was performed under light protection at 80°C for 4.5 h, without any mixing or shaking [18]. Control samples, containing only lignin and silver nitrate solutions separately, were also performed. After the reaction, the resulting solutions with the nanoparticles (hybrid lignin/AgNPs and the unreacted bulk reagents were not removed) were submitted to analysis of UV-visible spectroscopy, Dynamic Light Scattering (DLS) and Zeta Potential. For other analysis such as transmission electron microscopy (TEM) and Fourier-transformed infrared (FT-IR) spectroscopy, the resulting solutions of nanoparticles were dried at 45°C.

## 2.3. Nuclear Magnetic Resonance

The <sup>1</sup>H, <sup>13</sup>C and 2D HSQC nuclear magnetic resonance (NMR) analyses were recorded using a Bruker Advance DRX400 NMR spectrometer equipped with a 5-mm multinuclear inverse detection probe at 70°C. The base frequency was 400.13 and 100.63 MHz for <sup>1</sup>H and <sup>13</sup>C nuclei, respectively. For NMR analyses the lignin samples were dissolved in DMSO-*d*<sub>6</sub> [3,17], at 20 mg.mL<sup>-1</sup> for <sup>1</sup>H and HSQC and at 80 mg.mL<sup>-1</sup> for <sup>13</sup>C experiments.

Acquisition parameters were carried out using the pulse programs supplied with the Bruker manual. Chemical shifts are expressed relative to DMSO- $d_6$  at 39.51 ppm.

#### **2.4. Ultraviolet–visible spectrophotometry analysis**

The bio-reduction of Ag<sup>+</sup> ions with the different lignin solutions was monitored by absorbance measurement using an ultraviolet-visible (UV-Vis) spectrophotometer (Shimadzu, UV-1601 PC). The surface plasmon resonance (SPR) spectra of AgNPs in the samples were measured in the range between 200-800 nm with a resolution of 1 nm. The UV-vis spectra were recorded using a quartz cuvette and deionized water was used as reference.

#### **2.5. Fourier-transformed infrared spectroscopy**

Fourier Transform Infrared (FT-IR) Spectrometer (Bruker, Vertex 70) with DRIFT (diffuse reflectance) accessory was used for analysis of extracted lignins and synthesized AgNPs. Reflectance technique was used with 64 scans, resolution of 4 cm<sup>-1</sup>, without elimination of atmospheric compensation in the region between 4000 to 400 cm<sup>-1</sup>. The dried samples were mixed with potassium bromide (KBr) in a ratio of 1:5 using an agate mortar and pestle [20].

#### **2.6. TEM, DLS and Zeta Potential analysis of AgNPs**

The average hydrodynamic size of the AgNPs particles were determined by Dynamic Light Scattering (DLS) (Brookhaven, NanoDLS), after dilution 1:10. The morphology of AgNPs particles were analyzed by transmission electron microscopy (TEM) (JEOL, JEM 1200EX-II) operated at 120 kV. TEM samples were prepared by placing a drop of the suspension of hybrid lignin/AgNPs on carbon-coated copper grids and allowing water to evaporate at room temperature. Selected area electron diffraction (SAED) patterns were analyzed using the CrysTBox software in order to identify the silver crystal planes.

For Zeta potential analysis, the resulting solutions of hybrid lignin/AgNPs were diluted with ultrapure water in a ratio of 2:3 to give a total volume of 10 mL. The analyses were carried out using a Zeta Potential analyzer (Stabino) with a 10 mL PTFE measurement cell and a 400  $\mu\text{m}$  piston. The measurement of Zeta potential was done in a pH-titration mode using 0.05 mol.L<sup>-1</sup> HCl and 0.05 mol.L<sup>-1</sup> NaOH.

## 2.7. Antioxidant activity

The antioxidant activity was measured using 2,2-diphenyl-1-picrylhydrazyl (DPPH) as free radical. The lignin solutions were evaluated at concentrations of 200, 100, 50 and 25  $\mu\text{g.mL}^{-1}$ . In the case of the resulting solutions of hybrid lignin/AgNPs, the concentrations evaluated were 100, 50, 25 and 12.5% v/v, diluted in water. The reactions took place by mixing 0.2 mL of evaluated compound with 0.8 mL of 0.1 mmol.L<sup>-1</sup> DPPH (dissolved in methanol). The mixture was shaken vigorously and left to stand for 30 min in the dark before measuring the absorbance at 517 nm. Then, the scavenging ability was calculated using the following equation (1):

$$I(\%) = \left( \frac{A_{\text{control}} - A_{\text{sample}}}{A_{\text{control}}} \right) \cdot 100 \quad (\text{Eq. 1})$$

Where I (%) is the inhibition percent,  $A_{\text{control}}$  is the absorbance of the control reaction (containing water as sample) and  $A_{\text{sample}}$  is the absorbance of the test compound [21,22].

## 2.8. Antimicrobial activity

### 2.8.1. Disk diffusion susceptibility test

Bacterial sensitivity to antibiotics is commonly evaluated using a disk diffusion test. The antimicrobial activity was evaluated using the pathogenic bacteria *Escherichia coli* ATCC 35218 grown on Mueller-Hinton agar (MHA). Briefly, 100  $\mu\text{L}$  ( $10^8$  CFU.mL<sup>-1</sup>) of microbial culture were swabbed uniformly onto the individual plates using sterile cotton

swabs. Then, sterile paper disc (10 mm-diameter) containing 50  $\mu\text{L}$  of hybrid lignin/AgNPs solutions were placed on the MHA plates. The plates were incubated at 37°C for 24 h and the inhibition zones developed were further measured. Statistical analysis of data was carried out to determine the level of significance ( $P < 0.05$ ) by employing one-way analysis of variance (ANOVA) using Microsoft Excel 2013.

### 2.8.2. Minimum Inhibitory Concentration

The minimum inhibitory concentration (MIC) of AgNPs was determined according to the standard broth microdilution method against *E. coli* ATCC 25218 [23]. After 16 h, 30  $\mu\text{L}$  of resazurin ( $150 \mu\text{g}\cdot\text{mL}^{-1}$ ) were added to every well and the microplate was incubated one hour more. The development of a pink color indicated that no inhibitory activity at the tested concentration of antimicrobial agent was observed.

## 3. RESULTS AND DISCUSSION

Initially, the 2D HSQC NMR analyses showing the structural differences between the extracted lignins are presented. Sequentially, the AgNPs characterization results obtained by UV-Vis spectrophotometry, TEM, FT-IR spectroscopy, DLS, and Zeta potential are discussed. Finally, the results of antioxidant and antimicrobial activities of lignins and AgNPs are presented.

### 3.1. NMR characterization

The 2D HSQC NMR spectrum of a non-acetylated lignin (HAL1-L) sample with the main chemical structures is presented in **Fig. 2**. A comparison of the main  $^{13}\text{C}$ - $^1\text{H}$  correlation assignments for the four different lignins extracted from OPEFB under different conditions are listed in **Table 1**.

**Table 1.** HSQC NMR correlation assignments of non-acetylated lignin samples.

$\delta_C/\delta_H$				Assignment	Reference
HAL1-L	HAL2-L	HAL3-L	HAL4-L		
55.9/3.72	55.9/3.73	55.9/3.73	55.9/3.73	C-H in methoxyls (O-CH <sub>3</sub> )	[24]
59.6/3.72		59.6/3.70		A <sub>γ</sub> : C <sub>γ</sub> -H <sub>γ</sub> in β-O-4' substructures	[25]
72.2/4.87		72.2/4.87		A <sub>α</sub> : C <sub>α</sub> -H <sub>α</sub> in β-O-4' linked to a S units	[25]
86.0/4.13		86.0/4.12		A <sub>β</sub> : C <sub>β</sub> -H <sub>β</sub> in β-O-4' linked to a S unit	[25]
104.3/6.70		104.2/6.69	104.3/6.69	S <sub>2,6</sub> : C <sub>2,6</sub> -H <sub>2,6</sub> in S units	[26]
115.5/6.66		115.5/6.68		G <sub>5</sub> : C <sub>5</sub> -H <sub>5</sub> in G units	[24]
129.6/5.32	129.6/5.32	129.6/5.32	129.6/5.32	-CH=CH-	[24]

HSQC NMR spectra of lignin samples can be separated into three regions whose signals correspond to aliphatic, side-chain and aromatic/olefin <sup>13</sup>C-<sup>1</sup>H correlations. The aliphatic (non-oxygenated) region ( $\delta_C/\delta_H$  10-50/0.5-2.5 ppm) showed signals corresponding to -CH<sub>3</sub> and -CH<sub>2</sub> groups of the propyl chains and acetyl group in lignin [17]. These individual chemical shifts have been commonly observed in all lignin groups and consequently, do not allow the distinction between the units present in lignin [24].

The side-chain (also known as aliphatic oxygenated) region ( $\delta_C/\delta_H$  50-95/2.5-6.0 ppm) gives useful information about the different inter-unit linkages in OPEFB lignin. The most prominent signal at 55.9/3.73 ppm represented the methoxyl groups [24]. Other important signals corresponded to β-O-4' aryl ether linkages where C<sub>α</sub>-H<sub>α</sub> and C<sub>β</sub>-H<sub>β</sub> correlations were observed at  $\delta_C/\delta_H$  72.2/4.87 and 86.0/4.13 ppm for β-O-4' structures linked to S-lignin units, respectively. Also, the C<sub>γ</sub>-H<sub>γ</sub> correlations in β-O-4' substructures were observed at  $\delta_C/\delta_H$  59.6/3.70 ppm [25] (**Fig. 2 - structure A**).

It is important to mention that  $\beta$ -O-4' ether linkages were dramatically reduced during the biomass pretreatment process, as in the Kraft processes where the corresponding signals are not as predominant as the native lignins [27].

Phenylcoumaran structures and their degradation products, i.e. stilbene structures, were absent in all spectra. Moreover, no resinol nor dibenzodioxocin substructures were found in any spectra [27].

The main cross-signals found in the aromatic region ( $\delta_C/\delta_H$  95–160/5.5–8.5 ppm) corresponded principally to benzene rings of the lignin units, specifically from syringyl (S) lignin units. The  $C_{2,6}$ - $H_{2,6}$  correlation from the S-lignin unit exhibited a signal at  $\delta_C/\delta_H$  104.3/6.70 ppm [26] (**Fig. 2 - structure S**). Additionally, although a weak signal at  $\delta_C/\delta_H$  115.5/6.68 ppm could be attributed to the  $C_{5-10}$  correlation in found in G units [24], a strong correlation corresponding to  $C_{2-10}$  and  $C_6$ - $H_6$  was not found in any of the lignin samples (**Fig. 2 - structure G**). Although the signals of H-lignin units were not detected in the HSQC spectra, this information could be confirmed by Py-GC/MS analysis (**Fig. 2 - structure H**). The 2D HSQC NMR results showed that lignins obtained under harsh acid hydrolysis conditions (HAL2-L and HAL4-L, 3.5% acid for 60 min) exhibited less correlations compared to those obtained under mild acid hydrolysis conditions (HAL1-L and HAL3-L, 1.5% acid for 20 min) indicating higher degradation of the lignin complex structure.

### 3.2. Ultraviolet-visible spectrophotometry

The formation process of AgNPs using the four different lignins was confirmed by the change in color of the reaction solution from almost colorless to a yellowish color (**Fig. 3 –**

**Tubes**). This observed phenomenon was due to the excitation of surface plasmon vibrations in AgNPs [28].

The UV-Vis spectra of synthesized AgNPs (**Fig. 3**) were very different from the spectra of the corresponding lignins and AgNO<sub>3</sub> used as initial reagents. The spectra of the reaction solutions, at the beginning of the experiment, showed that the lignins in the samples are the major contributors of their absorbance values. After reaction, a strong and broad peak located between 420 and 440 nm was observed in the resulting AgNPs solutions. There was no clear difference in the peak position using the four different lignins. The maximum absorbance of the SPR peaks were found almost at the same wavelength (between 423 and 427 nm). The lower absorbance values indicated lower concentrations of AgNPs [29].

As the surface plasmon resonance peak of HAL1-L AgNPs presented the lowest absorbance value, it could indicate that lignin HAL1-L produced a much lower amount of AgNPs. Additionally, it was noticed that the lignins obtained under harsh conditions (HAL2-L and HAL4-L, using 3.5% acid for 60 min) produced higher amounts of AgNPs compared to those lignins obtained under mild conditions (HAL1-L and HAL3-L, using 1.5% acid for 20 min). These results suggested that lignins HAL2-L and HAL4-L presented higher reducing power than lignins HAL1-L and HAL3-L. Furthermore, the spectral position and width of SPR bands are influenced by size and shape of the prepared nanoparticles [30].

### **3.3. Fourier-Transformed Infrared spectroscopy**

The identification of specific functional groups in the synthesized AgNPs were also performed by FTIR. Remembering that lignin played two roles in the particle formation, as

capping and reducing agent. The characteristic absorption frequencies of lignin and AgNPs are reported in **Table 2**.

The strong and broad peaks at 3300-3400  $\text{cm}^{-1}$ , for the extracted lignins, indicated the presence of hydroxyl groups (O-H stretching) in aliphatic and aromatic structures [19]. The peaks located between 3000 and 2800  $\text{cm}^{-1}$  can be attributed to C-H aliphatic stretching in methoxyl (-OCH<sub>3</sub>), in methyl (-CH<sub>3</sub>) and methylene (=CH<sub>2</sub>/-CH<sub>2</sub>-) groups of the propyl side chain present in lignins [24]. The peaks in the range of 1758-1716  $\text{cm}^{-1}$  refer to the carbonyl (C=O) stretching vibrations [31]. The peaks between 1635-1595  $\text{cm}^{-1}$  and 1517-1509  $\text{cm}^{-1}$  were assigned to C=C stretching in the aromatic rings of S and G units in lignin, respectively [32,33] and the signals at 1458-1450  $\text{cm}^{-1}$  corresponded to asymmetric C-H deformations in -CH<sub>3</sub> and -CH<sub>2</sub>- [24]. The signals (1390-1330, 1224-1219 and 1126-1113  $\text{cm}^{-1}$ ) associated to syringyl and guaiacyl groups were also identified in all lignin samples and only some of those peaks were also observed in AgNPs spectra [34]. The peaks at 1056-1020  $\text{cm}^{-1}$  can be attributed to various vibrations like C-O, C-H and C=O [32]. It was not possible to find a notable difference between the four lignins extracted from OPEFB. In the case of lignin-mediated AgNPs, all of them presented the same functional groups. It was noticed that some signals from lignin samples did not appear on the AgNPs spectra, possibly due to electrostatic crosslinking between lignin and AgNPs [19].

Some authors proposed as mechanism of lignin-mediated AgNPs synthesis that the main functional groups involved in the reduction, capping and stability of AgNPs are the lignin carboxylic, aliphatic, and phenolic hydroxyl groups [35]. Additionally, under acidic and neutral conditions, silver ions can be directly reduced into AgNPs by lignin, without the formation of Ag<sub>2</sub>O as intermediate [36].

**Table 2.** FT-IR assignments of lignins and corresponding AgNPs.

Lignin Absorption bands (cm <sup>-1</sup> )	AgNPs Absorption bands (cm <sup>-1</sup> )	Type of bond	Reference
3317 – 3301	3428 – 3410	Aromatic and aliphatic O-H stretching	[19]
2934 – 2925	2931 – 2927	C-H aliphatic stretching in (-OCH <sub>3</sub> ), (-CH <sub>3</sub> ) and (-CH <sub>2</sub> /-CH <sub>2</sub> -) groups	[24]
2856 – 2849	2858 – 2852	C-H aliphatic stretching in (-OCH <sub>3</sub> ), (-CH <sub>3</sub> ) and (=CH <sub>2</sub> /-CH <sub>2</sub> -) groups	[24]
1721 – 1716	1768 – 1761	C=O (in carbonyl compounds)	[31]
1604 – 1595	1635 – 1622	C-H stretching in aromatic rings	[32,33]
1517 – 1509		C-H stretching in aromatic rings	[32,33]
1458 – 1450		C-H asymmetric deformations in -CH <sub>3</sub> and -CH <sub>2</sub> -	[24]
1352 – 1323	1393 – 1391	Syringyl ring breathing with C-O stretching	[34]
1224 – 1212		Guaiacyl ring breathing with C-O stretching	[34]
1120 – 1113	1125 – 1119	C-H in-plane deformation in syringyl	[34]
1027 – 1020	1056 – 1043	Various vibrations like C-O, C-H and C=O	[32]

### 3.4. TEM, DLS and Zeta potential analysis of AgNPs

In the bright field TEM mode, the dark spots revealed that the four lignin-mediated AgNPs possessed almost spherical morphology with very little agglomeration (**Fig. 4**). The shining spots on the dark field TEM mode showed metallic silver in the particles, confirming that most of them are real AgNPs. The selected area electron diffraction (SAED) pattern revealed the polycrystalline nature of the nanoparticles. The diffraction

rings, from inner to outer, corresponded to (111), (200) and (220) planes of face-centered cubic (fcc) structure of silver.

The four lignin-mediated AgNPs exhibited almost the same average hydrodynamic particle size, between 18 and 20 nm. **Fig. 5a** shows differences in the AgNPs size distribution. Well-dispersed AgNPs were found and the particles ranged in size from 1 to 40 nm. Additionally, the size of most of the particles from HAL1-L AgNP ranged between 15-20 nm, while the particles from HAL3-L and HAL4-L AgNP presented similar size distribution pattern with most of their particles ranging between 20-25 nm. In the case of HAL2-L AgNP, most of its particles are distributed between 15-25 nm. Another research reported AgNPs with higher average diameter (100 nm) using lignin extracted from *Acacia* wood powder as reducing agent [19]. Furthermore, AgNPs with average size between 20 and 23.6 nm were synthesized using alkali lignin [37]. Other AgNPs synthesized using *Coffea arabica* seed extract exhibited sizes ranging from 10 to 150 nm, depending on the amount of reducing agent added [11]. Moreover, purple heart plant leaf extract produced almost spherical AgNPs with average diameter of 98 nm [38]. Additionally, biosynthesized AgNPs using *Staphylococcus aureus* agglomerated and formed different nanostructures with particle sizes ranging from 160 to 180 nm [10].

The colloidal stability of AgNPs was characterized by Zeta potential. Generally, a nanoparticle suspension that exhibits an absolute Zeta potential lower than  $|20 \text{ mV}|$  is considered unstable, resulting in a particle phase separation from the solution [39]. On the contrary, a high absolute Zeta potential value designates a high electrical charge, causing a strong repulsive force among the particles for withholding agglomeration and phase separation [14].

As shown in **Fig. 5b**, the Zeta potential profiles exhibited by the four lignin-mediated AgNPs diluted in ultrapure water were almost the same. The differences observed between the four profiles could be principally attributed to a little higher concentration of unreacted silver ions present in samples such as HAL1-L AgNP and HAL3-L AgNP since Zeta potential could be affected by the solvent. The four lignin-mediated AgNPs possessed high stability in aqueous solution showing absolute Zeta potential values higher than 20 mV at pH values higher than 4.

Comparing with other manuscripts, AgNPs produced with lignin extracted from *Acacia* wood powder presented a Zeta potential value of -26.5 mV [19]. Additionally, AgNPs synthesized using *Citrus limon* (lemon) aqueous extract presented a Zeta potential of -29 mV at pH of 3.97 [40] and plant-mediated AgNPs using *Lantana camara* presented a Zeta potential ranging from -25 mV to -50 mV, as the amount of extract used in the synthesis increased [41].

As AgNPs were intended to be used in a complex solutions, such as culture media, the Zeta potential profiles were also examined diluting the AgNPs in Mueller-Hinton broth instead of ultrapure water. **Fig. 5b** showed that the four lignin-mediated AgNPs presented the same profile with Zeta potential values very close to 0 mV at pH values ranging from 2 to 10. This result implies that the AgNPs in solutions with higher ions content could result in colloidal instability, agglomeration of the particles and possible phase separation. Thus, agglomeration of AgNPs could explain a reduction of the physicochemical and biological properties such as a lower release of silver ions involved in antiseptic mechanisms [42,43].

Another important fact is that the AgNPs presented a negative Zeta potential at pH values higher than 5 and as their antimicrobial action stems from the localized emission of

$\text{Ag}^+$  ions at the cell membranes of microbes, their surface charge is probably the main facilitator of this biological activity [44]. Due to the negatively charged bacterial cell membranes, a charge inversion of the surface of AgNPs from negative to positive would be necessary and accomplished by functionalization of the surface of the nanoparticles [45].

### 3.5. Antioxidant activity

The antioxidant activities of the four lignins extracted from OPEFB and lignin-mediated AgNPs are shown in **Fig. 6**.

In **Fig. 6a**, it can be seen that the lignins extracted under harsh acid hydrolysis conditions (HAL2-L and HAL4-L, 3.5% acid for 60 min) exhibited higher scavenging activity than the lignins extracted under mild conditions (HAL1-L and HAL3-L, 1.5% acid for 20 min). This could be attributed to a higher amount of reducing functional groups on the chemical structure of lignins HAL2-L and HAL4-L. As the HSQC NMR results indicated a higher degradation of lignins HAL2-L and HAL4-L compared to HAL1-L and HAL3-L, it could also mean a higher amount of reducing functional groups in their structure. Additionally, the concentration of lignin that inhibited 50% of the free-radical ( $\text{IC}_{50}$ ) was calculated and presented in **Fig. 6b**. As stated above, lignins HAL2-L and HAL4-L exhibited higher reducing power than HAL1-L and HAL3-L.

Furthermore, from the reagents used for the synthesis of AgNPs, only lignin exhibited antioxidant capacity while silver nitrate did not exhibit any inhibitory capacity (data not presented). As the unreacted reagents from the AgNPs solutions were not removed to prepare a solution based only on AgNPs concentration, the antioxidant activity for the

diluted AgNPs solutions was expressed in terms of the lignin concentration used in their synthesis, as it is the reagent that would confer antioxidant capacity to the nanoparticles.

Making the dilutions from the resulting AgNPs solutions (100, 50, 25 and 12.5% v/v), the amount of lignin in the resulting solutions were approximately 40, 20, 10 and 5  $\mu\text{g}\cdot\text{mL}^{-1}$ . Therefore, the antioxidant activity of the resulting dilutions of the hybrid lignin/AgNPs was calculated. From **Fig. 6c**, it can be seen that the scavenging activity exhibited by the hybrid lignin/AgNP solutions corresponded to the lignin present in the solutions as their values were approximately the same as those exhibited by the lignin solutions alone. The functional groups on the surface of AgNPs could be responsible of the antioxidant capacity exhibited by the nanoparticles. As these functional groups came from lignin, it could be suggested that lignin conferred the antioxidant power to AgNPs.

### 3.6. Antimicrobial activity

The antibacterial activity of lignins,  $\text{AgNO}_3$  and AgNPs against *E. coli* was investigated. The disk-diffusion method was used to evaluate differences between the inhibition zones developed by the four different resulting solutions of hybrid lignin/AgNPs. The inhibition zones exhibited were  $19.3\pm 0.58$  mm,  $18.7\pm 0.6$  mm,  $18.7\pm 0.58$  mm, and  $18.7\pm 0.58$  mm for HAL1-L AgNP, HAL2-L AgNPs, HAL3-L AgNP, and HAL4-L AgNP, respectively. As no significant differences (P-value =0.44) were observed between the inhibition zones, HAL3-L AgNP was chosen to be evaluated by minimum inhibitory concentration (MIC) because the lignin used came from a mild hydrolysis process (1.5% acid for 20 min). HAL3-L AgNP resulting solution was dialyzed using a 1 kDa cut-off membrane and ultrapure water for 48 h.

For the minimum inhibitory concentration experiment, the four lignins, silver nitrate and HAL3-L AgNP were tested as antimicrobial agent in a 96-well microplate. All substances were tested at the same concentrations. In case of the four lignins tested, it was not possible to establish a MIC, since the microorganism was able to grow even at the highest concentration evaluated ( $1000 \mu\text{g.mL}^{-1}$ ). Besides evaluating MIC at higher concentration for lignin, other measurements should be made such as viable cells counting in order to know how much inhibition of cellular growth was exhibited by lignin.

On the contrary,  $\text{AgNO}_3$  exhibited a visible inhibitory effect even at the lowest concentrations tested ( $31.25 \mu\text{g.mL}^{-1}$ ). In case of the AgNPs solution (HAL3-L AgNP), it was possible to establish that a concentration of  $62.5 \mu\text{g.mL}^{-1}$  inhibited the visible growth of the microorganism tested (MIC). The difference in the MIC results between  $\text{AgNO}_3$  and AgNPs could be explained by the fact that most of  $\text{AgNO}_3$  in solution was already in ionic form or as soluble complex. It was ready available to interact with microorganisms, resulting in lower MIC values [46] whereas AgNPs behave like slow-release devices of silver ions that prolong the antimicrobial effect [42,43].

Additionally, the antimicrobial capacity of AgNPs depends mainly on physical and chemical properties such as shape, size, concentration and stability (Zeta potential) [47]. The lignin used in the synthesis of AgNPs may enhance the antimicrobial capacity. Generally, this synergistic effect is observed when the reducing agent also showed antimicrobial properties [48]. Thus, for the lignin used in this work, no antimicrobial activity was measured, at the concentrations tested against *E. coli*, and consequently, there was no synergistic effect on the antiseptic capacity of lignin-mediated AgNPs.

Compared to other works, AgNPs synthesized by microemulsion method exhibited a higher MIC values ( $100 \mu\text{g.mL}^{-1}$ ) [49], than in the current work. On the other hand, AgNPs

synthesized using fungal extracts exhibited a MIC of  $3.125 \mu\text{g.mL}^{-1}$  [23]. This lower MIC result was attributed to the binding of proteins to AgNPs, resulting in a synergistic effect in the antimicrobial activity.

So far, it is still not clear the antimicrobial mechanism of AgNPs. However, three well-defined mechanisms have been proposed: (1) through the release of reactive oxygen species (ROS) [50], (2) superficial contact between silver and microorganisms causing cell wall and membrane damage [29], and (3) penetration of AgNPs into the cell causing membrane damage and death of the organism [45]. Thus, a better understanding of the bactericidal action of the AgNPs would require an adequate examination of the membrane-bound and intracellular nanoparticles.

The size and shape control can promote the penetration of nanoparticles into the cell. Some authors have reported that nanoparticles in the range of 10-15 nm size could exhibit superior antimicrobial capacities than those of larger particle sizes [48]. This capacity was attributed to the large surface area of smaller nanoparticles, providing higher interaction area and increasing the intracellular penetration. In the present work, lignin-mediated nanoparticles showed average hydrodynamic particle size between 18 and 20 nm, small enough to penetrate in the cell membrane.

Additionally, as mentioned before, the Zeta potential values exhibited by AgNPs at pH higher than 5 were negative and very close to 0 mV, when dissolved in Mueller-Hinton broth (MHB). Based on this result, as the Coulombic interactions between AgNPs and the negatively charged bacterial cell membranes were not evident, there was no localized release of silver ions, reducing the antimicrobial effect. Thus, the charge inversion of the surface of the lignin-mediated AgNPs could result in higher antimicrobial activity [51].

It is worth to mention that lignin plays an important role not only as reducing agent but also as capping and stabilizing agent, preventing agglomeration of the particles (as shown in Zeta potential analyses), which may be useful in other applications. The use of lignin in the green synthesis of AgNPs may be advantageous over chemical methods because it may contribute with a reduced toxicity of the antimicrobial nanoparticles. Moreover, compared with other green methods such as plant extracts, the use of lignin present advantages such as resisting higher temperatures. Compared with the use of microorganisms, lignin recovery does not have to lead with the difficulties from manipulation of microorganisms.

The synthesis of AgNPs using lignin as reducing agent is an attractive idea considering that lignin has been considered, for a long time, as a residue produced in large quantities from the pulp and paper industry. Additionally, the recovery of lignin from OPEFB is also advantageous because it brings an environmental benefit and adds value to the agricultural waste. The present work presented the successful green synthesis of AgNPs using the lignin extracted under mild conditions (1.5% acid and 20 min) from OPEFB, reducing the energetic needs and costs of the extraction process and allowing the production of a value-added material with antioxidant and antimicrobial capacities. It is important to recall that AgNPs have been reported to be currently employed for their antiseptic properties in coatings, keyboards, washing machines, air-conditioners, wound dressings and biomedical devices [52–54]. However, many other applications, already mentioned in the introduction, highlight the potential and importance of silver in the nanoscale.

#### **4. CONCLUSIONS**

A green synthesis of AgNPs was obtained, using lignins, confirming our hypothesis. The 2D HSQC NMR analyses showed higher degradation of those lignins obtained under harsh

acid hydrolysis conditions and the silver nanoparticles were confirmed with aid of UV-vis and FT-IR spectroscopy, transmission electron microscopy, dynamic light scattering, and Zeta potential. The silver nanoparticles showed antioxidant activity attributed to the lignin used in the synthesis. In addition, the disk diffusion antimicrobial susceptibility test against *Escherichia coli* did not exhibit significant differences between the lignin-mediated silver nanoparticles. Furthermore, dialyzed HAL3-L AgNP showed a minimum inhibitory concentration of  $62.5 \mu\text{g.mL}^{-1}$ . These results confirm that lignin recovered from an agricultural residue can be successfully employed for value-added applications, such as green synthesis of silver nanoparticles, which are currently employed in different fields of science not only for its antiseptic properties.

#### **DECLARATION OF COMPETING INTEREST**

The authors declare that they have no conflict of interest.

#### **ACKNOWLEDGMENTS**

This work was supported by the Federal University of Paraná (UFPR), Aix-Marseille Université, Vale S.A., FINEP, CAPES, and CNPq. Special thanks to Laboratório de Biopolímeros (BioPol), Centro de Microscopia Eletrônica (CME-UFPR) and Centro de Ressonância Magnética Nuclear (RMN-UFPR) for the analysis performed in its facilities.

## REFERENCES

- [1] Indexmundi, Palm Oil Production by Country in 1000 MT, (2017).  
<https://www.indexmundi.com/agriculture/?commodity=palm-oil> (accessed December 15, 2018).
- [2] E.S. Hosseini, M.A. Wahid, Utilization of palm solid residue as a source of renewable and sustainable energy in Malaysia, *Renew. Sustain. Energy Rev.* 40 (2014) 621–632. <https://doi.org/10.1016/j.rser.2014.07.214>
- [3] J.D. Coral Medina, A. Woiciechowski, A. Zandora Filho, M.D. Nosedá, B.S. Kaur, C.R. Soccol, Lignin preparation from oil palm empty fruit bunches by sequential acid/alkaline treatment - A biorefinery approach, *Bioresour. Technol.* 194 (2015) 172–178. <https://doi.org/10.1016/j.biortech.2015.07.018>.
- [4] A. Tejado, C. Peña, J. Labidi, J. M. Echeverria, I. Mondragon, Physico-chemical characterization of lignins from different sources for use in phenol-formaldehyde resin synthesis, *Bioresour. Technol.* 98 (2007) 1655–1663.  
<https://doi.org/10.1016/j.biortech.2006.05.042>.
- [5] I.M. Chung, I. Park, K. Seung-Hyun, M. Thiruvengadam, G. Rajakumar, Plant-Mediated Synthesis of Silver Nanoparticles: Their Characteristic Properties and Therapeutic Applications, *Nanoscale Res. Lett.* 11 (2016) 1–14.  
<https://doi.org/10.1186/s11671-016-1257-4>.
- [6] K. Kurihara, C. Rockstuhl, T. Nakano, J. Tominaga, T. Arai, The size control of silver nano-particles in SiO<sub>2</sub> matrix film, *Nanotechnology.* 16 (2005) 1565–1568.  
<https://doi.org/10.1088/0957-4484/16/9/026>.

- [7] T.N. Jebakumar Immanuel Edison, M.G. Sethuraman, Electrocatalytic reduction of benzyl chloride by green synthesized silver nanoparticles using pod extract of *Acacia nilotica*, ACS Sustain. Chem. Eng. 1 (2013) 1326–1332.  
<https://doi.org/10.1021/sc4001725>.
- [8] G.A. Kahrilas, L.M. Wally, S.J. Fredrick, M. Hiskey, A.L. Prieto, J.E. Owens, Microwave-Assisted Green Synthesis of Silver Nanoparticles Using Orange Peel Extract, ACS Sustain. Chem. Eng. 2 (2014) 367–376.  
<https://doi.org/10.1021/sc4003664>.
- [9] N.H. Rao, L. N, S. V Pammi, P. Kollu, G. S, I. R, Green synthesis of silver nanoparticles using methanolic root extracts of *Diospyros paniculata* and their antimicrobial activities, Mater Sci Eng C Mater Biol Appl. 62 (2016) 553–557.  
<https://doi.org/10.1016/j.msec.2016.01.072>.
- [10] A. Nanda, M. Saravanan, Biosynthesis of silver nanoparticles from *Staphylococcus aureus* and its antimicrobial activity against MRSA and MRSE, Nanomedicine Nanotechnology, Biol. Med. 5 (2009) 452–456.  
<https://doi.org/10.1016/j.nano.2009.01.012>.
- [11] S.M. Navarro Gallón, E. Alpaslan, M. Wang, P. Larese-Casanova, M.E. Londoño, L. Atehortúa, J.J. Pavón, T.J. Webster, Characterization and study of the antibacterial mechanisms of silver nanoparticles prepared with microalgal exopolysaccharides, Mater. Sci. Eng. C. 99 (2019) 685–695. <https://doi.org/10.1016/j.msec.2019.01.134>.
- [12] R. Sanghi, P. Verma, Biomimetic synthesis and characterisation of protein capped silver nanoparticles, Bioresour. Technol. 100 (2009) 501–504.

<https://doi.org/10.1016/j.biortech.2008.05.048>.

- [13] V. Vilas, D. Philip, J. Mathew, Essential oil mediated synthesis of silver nanocrystals for environmental, anti-microbial and antioxidant applications, *Mater. Sci. Eng. C*. 61 (2016) 429–436. <https://doi.org/10.1016/j.msec.2015.12.083>.
- [14] D. Guo, D. Dou, L. Ge, Z. Huang, L. Wang, N. Gu, A caffeic acid mediated facile synthesis of silver nanoparticles with powerful anti-cancer activity, *Colloids Surfaces B Biointerfaces*. 134 (2015) 229–234. <https://doi.org/10.1016/j.colsurfb.2015.06.070>.
- [15] J.L. Castro-Mayorga, A. Martínez-Abad, M.J. Fabra, C. Olivera, M. Reis, J.M. Lagarón, Stabilization of antimicrobial silver nanoparticles by a polyhydroxyalkanoate obtained from mixed bacterial culture, *Int. J. Biol. Macromol.* 71 (2014) 103–110. <https://doi.org/10.1016/j.ijbiomac.2014.06.059>.
- [16] V. Dhand, L. Soumya, S. Blalacwaj, S. Chakra, D. Bhatt, B. Sreedhar, Green synthesis of silver nanoparticles using *Coffea arabica* seed extract and its antibacterial activity, *Mater. Sci. Eng. C*. 58 (2016) 36–43. <https://doi.org/10.1016/j.msec.2015.08.018>.
- [17] D.J. Coral Medina, A. Lorenci Woiciechowski, A. Zandona Filho, L. Bissoqui, M.D. Nosedá, L. Porto de Souza Vandenberghe, S. Faria Zawadzki, C.R. Soccol, Biological activities and thermal behavior of lignin from oil palm empty fruit bunches as potential source of chemicals of added value, *Ind. Crop. Prod.* 94 (2016) 630–637. <https://doi.org/10.1016/j.indcrop.2016.09.046>.
- [18] S. Hu, Y. Lo Hsieh, Silver nanoparticle synthesis using lignin as reducing and

- capping agents: A kinetic and mechanistic study, *Int. J. Biol. Macromol.* 82 (2016) 856–862. <https://doi.org/10.1016/j.ijbiomac.2015.09.066>.
- [19] K.R. Aadil, A. Barapatre, A.S. Meena, H. Jha, Hydrogen peroxide sensing and cytotoxicity activity of Acacia lignin stabilized silver nanoparticles, *Int. J. Biol. Macromol.* 82 (2016) 39–47. <https://doi.org/10.1016/j.ijbiomac.2015.09.072>.
- [20] K.J.P. Anthony, M. Murugan, M. Jeyaraj, N.K. Rathinam, G. Sangiliyandi, Synthesis of silver nanoparticles using pine mushroom extract: A potential antimicrobial agent against *E. coli* and *B. subtilis*, *J. Ind. Eng. Chem.* 20 (2014) 2325–2331. <https://doi.org/10.1016/j.jiec.2013.10.008>.
- [21] A. Saravanakumar, M. Ganesh, J. Jayaprakash, H.T. Jang, Biosynthesis of silver nanoparticles using *Cassia tora* leaf extract and its antioxidant and antibacterial activities, *J. Ind. Eng. Chem.* 28 (2015) 277–281. <https://doi.org/10.1016/j.jiec.2015.03.003>.
- [22] A. Lateef, M.A. Azeez, T.C. Asafa, T.A. Yekeen, A. Akinboro, I.C. Oladipo, L. Azeez, S.E. Ajibade, S.A. Ojo, E.B. Gueguim-kana, L.S. Beukes, Biogenic synthesis of silver nanoparticles using a pod extract of *Cola nitida*: Antibacterial and antioxidant activities and application as a paint additive, *Integr. Med. Res.* 10 (2016) 551–562. <https://doi.org/10.1016/j.jtusci.2015.10.010>.
- [23] M.D. Balakumaran, R. Ramachandran, P. Balashanmugam, D.J. Mukeshkumar, P.T. Kalaichelvan, Mycosynthesis of silver and gold nanoparticles: Optimization, characterization and antimicrobial activity against human pathogens, *Microbiol. Res.* 182 (2016) 8–20. <https://doi.org/10.1016/j.micres.2015.09.009>.

- [24] S.K. Singh, P.L. Dhepe, Isolation of lignin by organosolv process from different varieties of rice husk: Understanding their physical and chemical properties, *Bioresour. Technol.* 221 (2016) 310–317. <https://doi.org/10.1016/j.biortech.2016.09.042>.
- [25] M.F. Li, S.N. Sun, F. Xu, R.C. Sun, Formic acid based organosolv pulping of bamboo (*Phyllostachys acuta*): Comparative characterization of the dissolved lignins with milled wood lignin, *Chem. Eng. J.* 179 (2012) 80–89. <https://doi.org/10.1016/j.cej.2011.10.060>.
- [26] Q. Schmetz, G. Maniet, N. Jacquet, H. Teramura, C. Ogino, A. Kondo, A. Richel, Comprehension of an organosolv process for lignin extraction on *Festuca arundinacea* and monitoring of the cellulose degradation, *Ind. Crop. Prod.* 94 (2016) 308–317. <https://doi.org/10.1016/j.indcrop.2016.09.003>.
- [27] C. Fernández-Costas, S. González, M.A. Sanromamán, D. Moldes, Structural characterization of kraft lignins from different spent cooking liquors by 1D and 2D Nuclear Magnetic Resonance spectroscopy, *Biomass and Bioenergy.* 63 (2014) 156–166. <https://doi.org/10.1016/j.biombioe.2014.02.020>.
- [28] S. Mohan, O.S. Oluwafemi, S.C. George, V.P. Jayachandran, F.B. Lewu, S.P. Songca, N. Kalarikkal, S. Thomas, Completely green synthesis of dextrose reduced silver nanoparticles, its antimicrobial and sensing properties, *Carbohydr. Polym.* 106 (2014) 469–474. <https://doi.org/10.1016/j.carbpol.2014.01.008>.
- [29] Y.S. Chan, M. Mat Don, Biosynthesis and structural characterization of Ag nanoparticles from white rot fungi, *Mater. Sci. Eng. C.* 33 (2013) 282–288.

<https://doi.org/10.1016/j.msec.2012.08.041>.

- [30] S.L. Smitha, K.M. Nissamudeen, D. Philip, K.G. Gopchandran, Studies on surface plasmon resonance and photoluminescence of silver nanoparticles, *Spectrochim. Acta - Part A Mol. Biomol. Spectrosc.* 71 (2008) 186–190.  
<https://doi.org/10.1016/j.saa.2007.12.002>.
- [31] R. El Hage, N. Brosse, L. Chrusciel, C. Sanchez, P. Sannigrahi, A. Ragauskas, Characterization of milled wood lignin and ethanol organosolv lignin from *miscanthus*, *Polym. Degrad. Stab.* 94 (2009) 1632–1638.  
<https://doi.org/10.1016/j.polymdegradstab.2009.07.007>.
- [32] R.J.A. Gosselink, A. Abächerli, H. Semke, R. Malherbe, P. Käuper, A. Nadif, J.E.G. Van Dam, Analytical protocols for characterisation of sulphur-free lignin, *Ind. Crops Prod.* 19 (2004) 271–281. <https://doi.org/10.1016/j.indcrop.2003.10.008>.
- [33] I. Carrillo, R.T. Mendonça, M. A. go, O.J. Rojas, Comparative study of cellulosic components isolated from different Eucalyptus species, *Cellulose.* 25 (2018) 1011–1029. <https://doi.org/10.1007/s10570-018-1653-2>.
- [34] A. Toledano, L. Serrano, A. Garcia, I. Mondragon, J. Labidi, Comparative study of lignin fractionation by ultrafiltration and selective precipitation, *Chem. Eng. J.* 157 (2010) 93–99. <https://doi.org/10.1016/j.cej.2009.10.056>.
- [35] R.G. Saratale, G.D. Saratale, G. Ghodake, S.K. Cho, A. Kadam, G. Kumar, B.H. Jeon, D. Pant, A. Bhatnagar, H.S. Shin, Wheat straw extracted lignin in silver nanoparticles synthesis: Expanding its prophecy towards antineoplastic potency and hydrogen peroxide sensing ability, *Int. J. Biol. Macromol.* 128 (2019) 391–400.

<https://doi.org/10.1016/j.ijbiomac.2019.01.120>.

- [36] S. Hu, Y. Lo Hsieh, Silver nanoparticle synthesis using lignin as reducing and capping agents: A kinetic and mechanistic study, *Int. J. Biol. Macromol.* 82 (2016) 856–862. <https://doi.org/10.1016/j.ijbiomac.2015.09.066>.
- [37] Y. Xue, X. Qiu, Z. Liu, Y. Li, Facile and Efficient Synthesis of Silver Nanoparticles Based on Biorefinery Wood Lignin and Its Application as the Optical Sensor, *ACS Sustain. Chem. Eng.* (2018). <https://doi.org/10.1021/acssuschemeng.8b00578>.
- [38] M.S. Hasnain, M.N. Javed, M.S. Alam, P. Rishishwar, S. Rishishwar, S. Ali, A.K. Nayak, S. Beg, Purple heart plant leaves extract-mediated silver nanoparticle synthesis: Optimization by Box-Behnken design, *Mater. Sci. Eng. C.* 99 (2019) 1105–1114. <https://doi.org/10.1016/j.msec.2019.02.061>.
- [39] Q. Sun, X. Cai, J. Li, M. Zhang, Z. Chen, C.P. Yu, Green synthesis of silver nanoparticles using tea leaf extract and evaluation of their stability and antibacterial activity, *Colloids Surfaces A Physicochem. Eng. Asp.* 444 (2014) 226–231. <https://doi.org/10.1016/j.colsurfa.2013.12.065>.
- [40] T.C. Prathna, N. Chandrasekaran, A.M. Raichur, A. Mukherjee, Biomimetic synthesis of silver nanoparticles by *Citrus limon* (lemon) aqueous extract and theoretical prediction of particle size, *Colloids Surfaces B Biointerfaces.* 82 (2011) 152–159. <https://doi.org/10.1016/j.colsurfb.2010.08.036>.
- [41] B. Ajitha, Y. Ashok Kumar Reddy, P. Sreedhara Reddy, Green synthesis and characterization of silver nanoparticles using *Lantana camara* leaf extract, *Mater.*

- Sci. Eng. C. 49 (2015) 373–381. <https://doi.org/10.1016/j.msec.2015.01.035>.
- [42] C. Greulich, S. Kittler, M. Epple, G. Muhr, M. Köller, Studies on the biocompatibility and the interaction of silver nanoparticles with human mesenchymal stem cells (hMSCs), *Langenbeck's Arch. Surg.* 394 (2009) 495–502. <https://doi.org/10.1007/s00423-009-0472-1>.
- [43] K.K. Comfort, E.I. Maurer, S.M. Hussain, Slow release of ions from internalized silver nanoparticles modifies the epidermal growth factor signaling response, *Colloids Surfaces B Biointerfaces.* 123 (2014) 136–142. <https://doi.org/10.1016/j.colsurfb.2014.09.008>
- [44] A.P. Richter, J.S. Brown, B. Bharti, A. Wang, S. Gangwal, K. Houck, E.A. Cohen Hubal, V.N. Paunov, S.D. Stoyanov, O.D. Velev, An environmentally benign antimicrobial nanoparticle based on a silver-infused lignin core, *Nat. Nanotechnol.* 10 (2015) 817–823. <https://doi.org/10.1038/nnano.2015.141>.
- [45] A. Ravindran, P. Charanraj, S.S. Khan, Biofunctionalized silver nanoparticles: Advances and prospects, *Colloids Surfaces B Biointerfaces.* 105 (2013) 342–352. <https://doi.org/10.1016/j.colsurfb.2012.07.036>.
- [46] S. Zhang, L. Liu, V. Pareek, T. Becker, J. Liang, S. Liu, Effects of broth composition and light condition on antimicrobial susceptibility testing of ionic silver, *J. Microbiol. Methods.* 105 (2014) 42–46. <https://doi.org/10.1016/J.MIMET.2014.07.009>.
- [47] M. Jeyaraj, S. Varadan, K.J.P. Anthony, M. Murugan, A. Raja, S. Gurunathan, Antimicrobial and anticoagulation activity of silver nanoparticles synthesized from

- the culture supernatant of *Pseudomonas aeruginosa*, J. Ind. Eng. Chem. 19 (2013) 1299–1303. <https://doi.org/10.1016/j.jiec.2012.12.031>.
- [48] A. Roy, O. Bulut, S. Some, A.K. Mandal, M.D. Yilmaz, Green synthesis of silver nanoparticles: Biomolecule-nanoparticle organizations targeting antimicrobial activity, RSC Adv. 9 (2019) 2673–2702. <https://doi.org/10.1039/c8ra08982e>.
- [49] I.A. Wani, S. Khatoon, A. Ganguly, J. Ahmed, T. Ahmad, Structural characterization and antimicrobial properties of silver nanoparticles prepared by inverse microemulsion method, Colloids Surfaces B Biointerfaces. 101 (2013) 243–250. <https://doi.org/10.1016/j.colsurfb.2012.07.001>
- [50] A.E. Nel, L. Mädler, D. Velegol, T. Xia, E. J. V Hoek, P. Somasundaran, F. Klaessig, V. Castranova, M. Thompson, Understanding biophysicochemical interactions at the nano–bio interface, Nat. - Mater. 8 (2009) 543–557. <https://doi.org/10.1038/nmat2447>.
- [51] A.A. Yaqoob, H. Ahmad, F. Parveen, A. Ahmad, M. Oves, I.M.I. Ismail, H.A. Qari, K. Umar, M.N. Mohammad Ibrahim, Recent Advances in Metal Decorated Nanomaterials and Their Various Biological Applications: A Review, Front. Chem. 8 (2020) 1–23. <https://doi.org/10.3389/fchem.2020.00341>.
- [52] A. Singh, K. Kaur, Biological and Physical Applications of Silver Nanoparticles with Emerging Trends of Green Synthesis, Silver Nanoparticles - Heal. Saf. [Working Title]. (2019). <https://doi.org/10.5772/intechopen.88684>.
- [53] J. Jeevanandam, A. Barhoum, Y.S. Chan, A. Dufresne, M.K. Danquah, Review on nanoparticles and nanostructured materials: History, sources, toxicity and

regulations, Beilstein J. Nanotechnol. 9 (2018) 1050–1074.

<https://doi.org/10.3762/bjnano.9.98>.

- [54] S. Ahmed, M. Ahmad, B.L. Swami, S. Ikram, A review on plants extract mediated synthesis of silver nanoparticles for antimicrobial applications: A green expertise, J. Adv. Res. 7 (2016) 17–28. <https://doi.org/10.1016/j.jare.2015.02.007>.

Journal Pre-proof

**Figure captions**

**Figure 1.** Extraction sequence of lignin from oil palm empty fruit bunches.

**Figure 2.** HSQC NMR spectrum of HAL1-L lignin with main chemical structures: (A)  $\beta$ -O-4' aryl ether linkages; (S) syringyl units; (G) guaiacyl units and (H) *p*-hydroxyphenil units.

**Figure 3.** UV-Vis spectra of surface plasmon resonance for AgNPs using four different lignins: a) HAL1-L; b) HAL2-L; c) HAL3-L and d) HAL4-L. *Red: AgNPs solution after 4.5 h of reaction; Blue: AgNPs solution at the beginning of the reaction; Green: Lignin solution; Yellow: AgNO<sub>3</sub> solution.*

**Figure 4.** TEM images of AgNPs.

**Figure 5.** Dynamic light scattering and Zeta potential. a) Particle size distribution of AgNPs, b) Zeta potential as a function of pH for AgNPs in ultrapure water and in Mueller-Hinton broth (MHB).

**Figure 6.** Antioxidant activity (DPPH): (a) Scavenging activity of lignins at different concentrations; (b) Inhibitory concentration of 50% of free-radical by different lignins; (c) Scavenging activity of diluted resulting solutions from the synthesis of AgNPs (100, 50, 25 and 12.5%) expressed in lignin content.

Figure 1

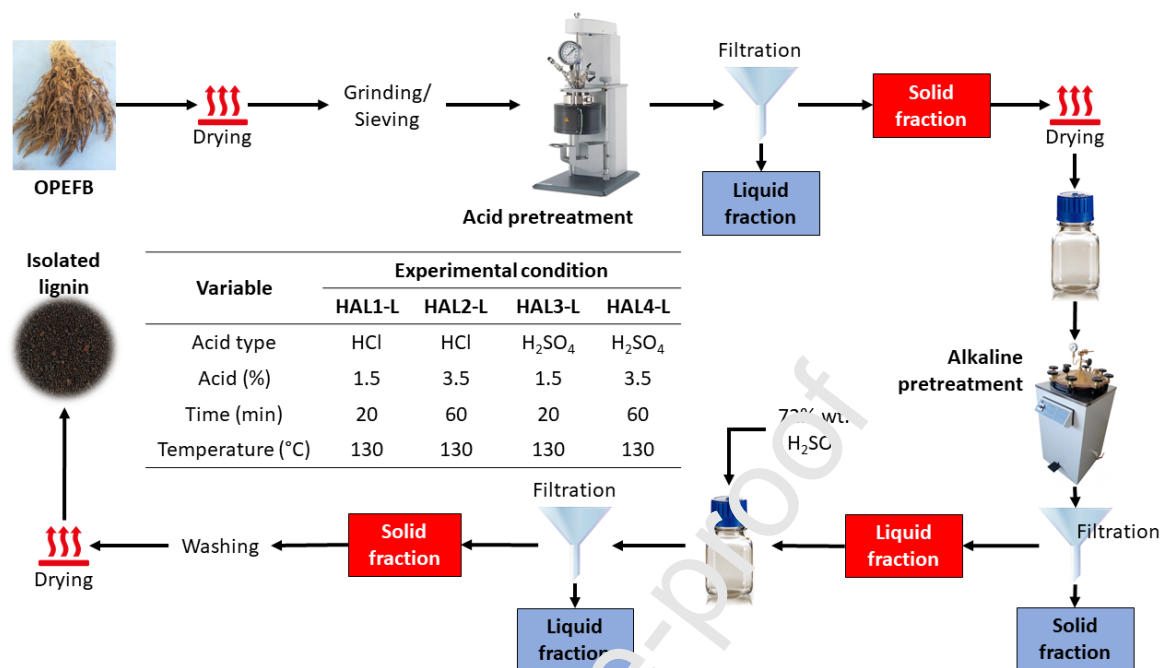


Figure 2

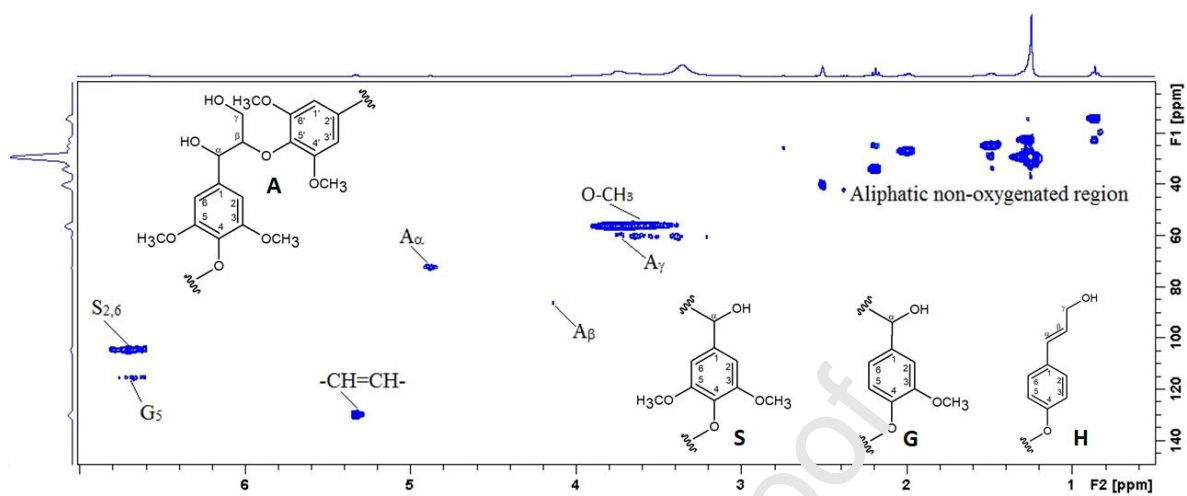


Figure 3

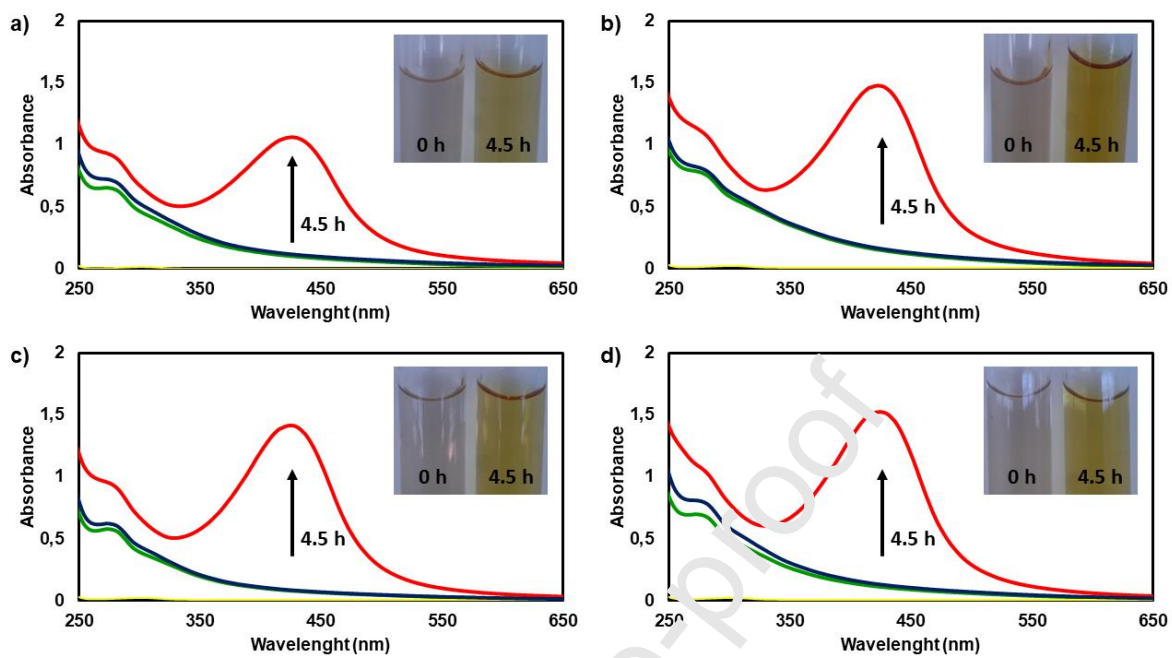


Figure 4

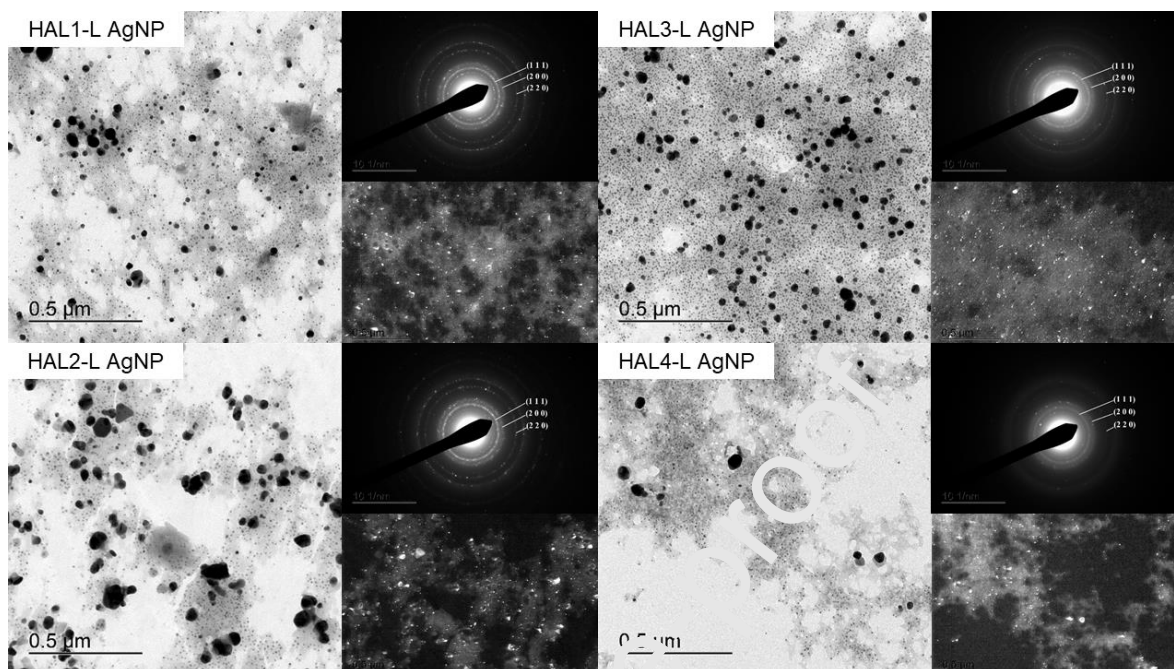


Figure 5

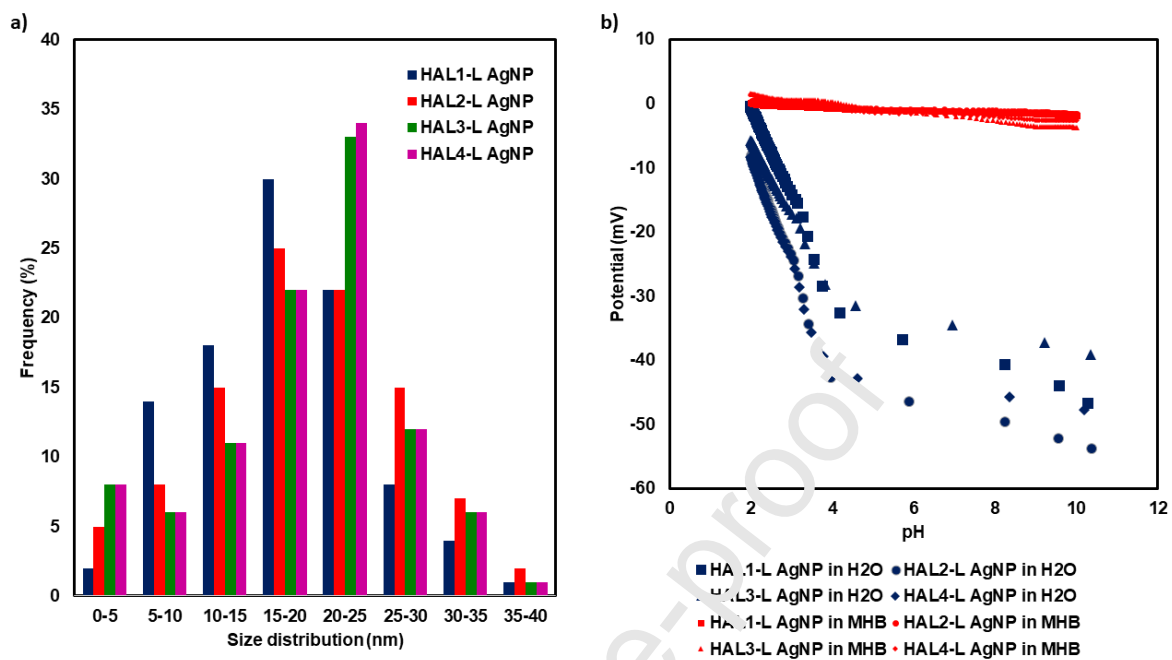
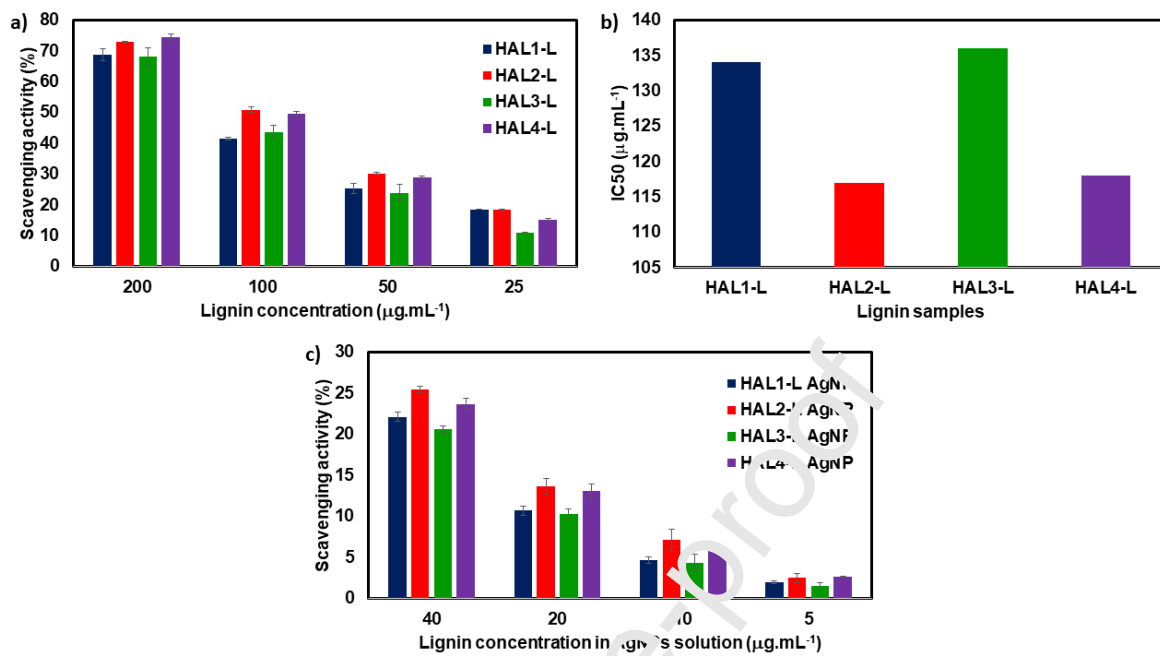


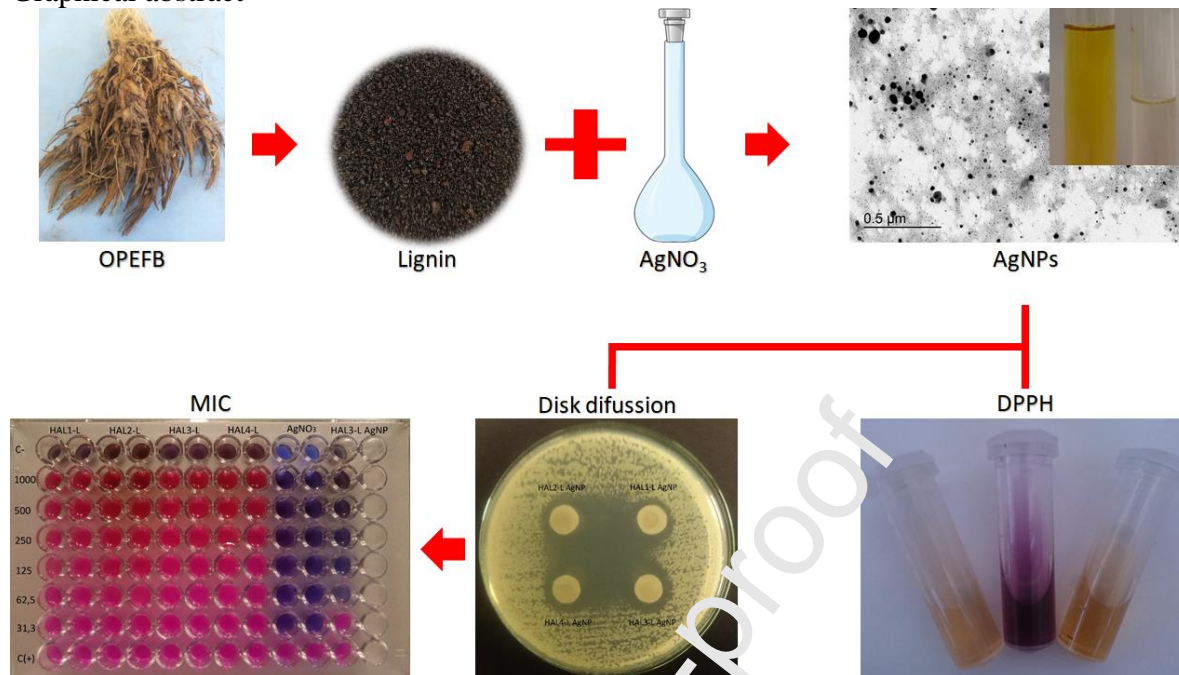
Figure 6



**CRedit author statement**

**Luis Alberto Zevallos Torres:** Methodology, Formal analysis, Investigation, Data curation, Writing – Original Draft, Writing – Review & Editing. **Adenise Lorenci Woiciechowski:** Supervision, Resources, Writing – Original Draft, Writing – Review & Editing. **Valcineide Oliveira de Andrade Tanobe:** Supervision, Investigation, Data curation, Writing – Original Draft. **Arion Zandona Filho:** Resources, investigation. **Rilton Alves de Freitas:** Supervision, Resources, Data curation, Writing – Original Draft. **Miguel Daniel Nosedá:** Supervision, Resources, Data curation, Writing – Original Draft. **Erico Saito Szameitat:** Data curation, Writing – Original Draft. **Craig Faulds:** Writing – Original Draft, Writing – Review & Editing. **Pedro Coutinho:** Writing – Original Draft, Writing – Review & Editing. **Emanuel Bertolino:** Writing – Original Draft, Writing – Review & Editing. **Carlos Ricardo Socol:** Resources, Writing – Original Draft, Writing – Review & Editing, Funding Acquisition.

Graphical abstract



Journal Pre-proof

**Highlights:**

- Lignins were extracted from oil palm empty fruit bunches at different conditions.
- Green synthesis of silver nanoparticles using different lignins.
- AgNPs showed scavenging activities attributed to lignin contributions.
- AgNPs displayed a minimum inhibitory concentration of 62.5  $\mu\text{g.L}^{-1}$  against *E. coli*.

Journal Pre-proof